Gümüşhane University Journal of Science

GUFBD / *GUJS* (2025) 15(4): 1179-1193 doi: 10.17714/gumusfenbil.1728851 Research Article

Forensic and analytical profiling of ignitable liquid residues on diverse fabric types

Çeşitli kumaş türleri üzerindeki tutuşabilir sıvı kalıntılarının adli ve analitik profilinin araştırılması

Soner KIZIL*[1,2], Buse Ilgım YOSMAOĞLU[1], Sevil ATASOY[1,2,3],

[1]*Üsküdar Üniversitesi, Mühendislik ve Doğa Bilimleri Fakültesi, Adli Bilimler Bölümü, 34662, İstanbul*

[2]*Üsküdar Üniversitesi, Bağımlılık ve Adli Bilimler Enstitüsü,34662, İstanbul*

[3]*Birleşmiş Milletler Uluslararası Narkotik Kontrol Kurulu, Viyana, Avusturya*

• Received: 27.06.2025 • Accepted: 01.12.2025

Abstract

Ignitable liquids (IL)s are crucial evidence in forensic fire investigations to determine the origin and cause of a fire. This study aimed to identify the type of accelerant used by examining the chemical changes in samples obtained from six different textile fabrics (wool, cotton, polyester, polyacrylic, polyamide and acetate) that were unburned, burned without accelerant, and burned with various ignitable liquids (kerosene, synthetic thinner, ethanol, and gasoline), using Fourier Transform Infrared Spectroscopy (FTIR) and Principal Component Analysis (PCA). The analyses determined that each ignitable liquid left distinguishable chemical traces on the fabrics with its unique characteristic FTIR bands. The study reveals that FTIR analyses supported by the PCA method can be considered a supplementary, rapid, and non-destructive technique for ignitable liquid detection in forensic fire investigations, providing additional support to standard Gas Chromatography-Mass Spectrometry (GC-MS) analysis used in routine analyses.

Keywords: Fire, Forensic fire investigations, FTIR, Ignitable liquid analysis, PCA, Textile fibers

Öz

Yanıcı sıvılar, adli yangın incelemelerinde yangının başlangıç noktasını ve nedenini belirlemek için kullanılan kritik delillerden biridir. Bu çalışmada, altı farklı tekstil kumaşının (yün, pamuk, polyester, poliakrilik, poliamid ve asetat) yanmamış, yanıcısız yakılmış ve çeşitli yanıcı sıvılarla (gazyağı, tiner, etil alkol ve benzin) yakılarak elde edilen numunelerdeki kimyasal değişikliklerin Fourier Dönüşümlü Kızılötesi Spektroskopisi (FTIR) ve Temel Bileşen Analizi (PCA) ile incelenerek kullanılan yanıcının türünün tespiti amaçlanmıştır. Analizler, her bir yanıcı sıvının kumaşlar üzerinde kendine özgü karakteristik FTIR pikleriyle ayırt edilebilir kimyasal izler bıraktığını ortaya koymuştur. Çalışma, PCA yöntemiyle desteklenen FTIR analizlerinin adli yangın incelemelerinde yanıcı sıvı tayininde rutin analizlerde kullanılan standart Gaz Kromatografisi-Kütle Spektrometresi (GC-MS) analizine ek destekleyici, hızlı ve tahribatsız bir yöntem olarak değerlendirilebileceğini ortaya koymaktadır.

Anahtar kelimeler: *Yangın, Adli yangın incelemeleri, FTIR, Yanıcı sıvı analizi, PCA, Tekstil lifleri*

1. Introduction

Fire is a rapid, self-sustaining oxidation process, typically involving combustible materials reacting with an oxidizing agent that produces heat, light, and various combustion products. While inherently a chemical reaction, the precise behavior and propagation of fire are significantly influenced by the physical state, distribution, and environmental conditions of the fuel, integrating principles from chemistry, heat transfer, and fluid dynamics. This phenomenon can range from controlled processes used for energy and heating to destructive, uncontrolled events (Drysdale, 2011). There are different combustion element models that explain the basic elements necessary for the formation of a fire, such as the fire triangle, fire quadrilateral, fire pentagon and the life cycle of fire. Although there are different models describing fire formation, the most widely accepted model is the fire triangle. The fire triangle model states that three key factors must

*Soner KIZIL; soner.kizil@uskudar.edu.tr, snrkzl@gmail.com

constantly interact for fire to occur; combustible, oxidizing agent and heat. If one of these three conditions does not occur, the fire goes out (Stauffer et al., 2006a). Combustibles are chemically capable of being oxidized, meaning they will ignite if a proper ignition source is present. Combustibles can be found in different molecular structures, organic or inorganic, in three basic states of matter (Stauffer et al., 2006a). Typically, atmospheric oxygen serves as the primary oxidizing agent in most combustion cases. However, fires can also ignite and sustain themselves without oxygen from the air if fuels combine with chemical oxidizers-(NFPA, 2021).

Heat is the thermal energy required to initiate and sustain combustion. It represents the energy required to raise the fuel temperature, facilitate the release of flammable vapors, and achieve ignition. Beyond initial ignition, heat plays a critical role in the spread and growth of a fire by continuing a continuous feedback loop which vaporizes more fuel, which in turn spreads and intensifies the flame (NFPA, 2021). The heat source can be an exothermic reaction, or various other types of ignition sources such as electrical, biological, mechanical, or nuclear (Stauffer et al., 2006a). Fire is the macroscopic manifestation of combustion. Combustion is an exothermic chemical reaction in which a fuel undergoes rapid oxidation in the presence of an oxidizer, most cases oxygen, releasing heat and light as well as a range of combustion products such as carbon dioxide, water vapor, and other byproducts that depend on the fuel composition (Quintiere, 2006). Fires are divided into two main categories, natural and human-made, based on their causes. Natural fires are fires that occur naturally without human intervention and are caused by events such as lightning, drought, earthquakes, and volcanic activity, the most common of which is lightning (U.S. Bureau of Indian Affairs, 2024). On the other hand, human-caused fires occur for a variety of reasons, such as carelessness, negligence, unconscious fire starting, vehicles, electrical problems and arson (Balch et al., 2017). At the international level, various fire classification system standards have been developed, such as NFPA-10, ISO 3941, AS/NZS 1850 and DIN EN2. According to NFPA 10-Standard for Portable Fire Extinguishers book; Class A fires are fires in ordinary combustible materials, such as wood, cloth, paper, rubber, and many plastics. Class B fires are fires in flammable liquids, combustible liquids, and flammable gases. Class C fires are fires that involve energized electrical equipment. Class D fires are fires in combustible metals, such as magnesium, titanium, zirconium, sodium, lithium, and potassium. Class K fires are fires in cooking appliances that involve combustible cooking media (vegetable or animal oils and fats) (NFPA, 2022). While classification systems focus primarily on the type of fuel involved in fires, forensic and clinical psychology literature makes distinctions on fire-starting behaviors (Burton et al., 2012). Fire-starting behaviors are described by a variety of terms, the distinction between these terms is important in defining criminality in the criminal justice system and for fire prevention purposes. These terms are fire setting, arson and pyromania. Fire setting is the act of setting fires, which can be accidental or intentional, and is independent of the person's intention (Segal et al., 2024). Arson is defined as setting fire to a valuable object or property with the intent to harm or with any unlawful intent (Yadav et al., 2020). Pyromania is a psychiatric disorder that usually begins in childhood and can persist throughout life, characterized by an uncontrollable urge to set a deliberate, purposeful fire and intense pleasure or relief from doing so (Segal et al., 2024).

Arson is a serious problem everywhere, causing significant harm and negatively affecting not only the individual but also the community health, safety and the national economy (Segal et al., 2024). There were 65,053 reported arson cases in the UK between January 2022 and December 2024, with 4.83% of these resulting in the suspect being charged (Palmer, 2024). The annual cost of arson fires in England and Wales is estimated at £2.1 billion (Association of British Insurers, 2004). In 2022, the civilian death rate from fires in the United States is recorded at 11.4 per million people (U.S. Fire Administration, 2023) and a total of 25,345 arson cases were officially reported and submitted to the FBI database (Federal Bureau of Investigation, 2024). The arson attack on France's high-speed rail network, which took place just before the opening ceremony of the 2024 Paris Olympic Games, affected an estimated 800,000 people due to delays (CNBC, 2024). In the Australian state of New South Wales, there are 1,500-3,000 arson attacks each year, causing approximately $25 million worth of damage, but only about 10 people are convicted of arson each year (Hall, 1988). As is evident from examples such as these, arson cases cause huge losses on a global scale and must be investigated carefully.

In many arson cases, ignitable liquids are used as accelerants to initiate the fire, and they are considered key indicators in fire debris analysis (Sampat et al., 2018). The definition of ignitable liquid is based on the physical and chemical properties of a material and includes flammable and combustible liquids. The term accelerant refers to a fuel or oxidizer that is intentionally used to start, grow, or increase the rate at which a

fire spreads; therefore, it is defined as an accelerant depending on how it is used. Although accelerants are usually ignitable liquids there can be different types of accelerants (NFPA, 2021; Stauffer et al., 2006b). The most used accelerants are petroleum products, their derivatives and organic volatile liquids. Gasoline is the most commonly used accelerant due to its easy accessibility, low cost, and high energy content that promotes rapid fire spread. In addition to gasoline, other ignitable liquids can also be used to initiate fires, such as thinners, lamp oils, fuels, alcohols, and certain solvents (Stauffer et al., 2006b). Gasoline is a branched and straight-chain alkane composed of low molecular weight aliphatic and aromatic hydrocarbons with carbon numbers ranging from C4–C12. Ethyl alcohol is a primary alcohol with the formula C_2H_5OH. Kerosene consists of aliphatic hydrocarbons with carbon chains ranging from C10–C16. Thinner is a liquid used in the dilution of chemicals such as paint, mainly containing toluene, xylene and acetate derivatives, and its variable content leads to different peak combinations in the FTIR spectrum of thinner (Kuppusamy et al., 2020).

Combustible liquids possess a closed-cup flash point (i.e., the lowest temperature at which a liquid will release sufficient vapor to cause a spontaneous ignition at its surface, under specified conditions) at or above 37.8°C. Flammable liquid possess a closed-cup flash point below 37.8°C (NFPA, 2021). According to the NFPA liquid classification scheme, flammable liquids are classified as Class I Liquids while combustible liquids are classified as Class II and Class III Liquids. Specifically, Class II Liquids exhibit a closed-cup flash point at or above 37.8°C but below 60°C, and Class III Liquids have a closed-cup flash point at or above 60°C. Gasoline (flash point approximately −40°C), 96% pure ethanol (≈13°C), thinner with the main components toluene (≈4°C) and xylene (≈27°C) are in the Class I – Flammable Liquids category of NFPA liquid classification scheme due to their flash point below 37.8°C, while kerosene with a flash point ranging from 38°C to 72°C is in the Class II/III – Combustible Liquids category (NFPA, 2024). Since three of the liquids used in this experiment were flammable and one was combustible, the term ignitable liquid was used to include all of them. Molotov cocktails, which are frequently used in arson cases, are simple incendiary devices that usually contain various chemicals, such as IL, placed in a glass bottle and a piece of cloth that acts as a wick (Evans-Nguyen & Hutches, 2019). During the attack, the fabric wick is ignited and thrown away, when the bottle is broken, the IL spreads and ignites rapidly, starting the fire (Mandal et al., 2021). In such cases, forensic fabric fiber analysis is of great importance, as the examination of burnt textile fibers detected in the fire scene analysis provides valuable information about the way the fire was started and whether the fire was intentional or accidental (Williams, 2018).

Textile fibers are essentially polymers formed by monomers specific to each fiber type, which are linked together in a type-specific bonding arrangement (Peterson, 2015). Fibers are broadly classified into two classes: natural and synthetic. Natural fibers are fibers that produced from natural materials and are divided into three subgroups: plant-based cellulosics such as cotton and linen, animal protein-based such as wool and silk, and mineral-based such as asbestos. Manufactured fibers are fibers produced by man made using natural polymers or synthetic chemicals and they are divided into 2 subgroups; regenerated fibers, that is, fibers containing organic polymers, are obtained by various chemical processes such as viscose and acetate, synthetic fibers produced by polymerization from synthetic chemical polymers such as polyamide, polyester and polyacrylic (Mather et al., 2023). In forensic textile fiber analysis, non-destructive methods are preferred because very small amounts of fiber are typically recovered from crime scenes. Therefore, the first choice in the identification of fibers is microscopic examination (Houck, 2009; Smith, 2011). FTIR spectroscopy is also an important analysis method used in forensic fiber analysis as a non-destructive technique (Li, 2007; Rouessac & Rouessac, 2013). FTIR spectroscopy uses the interaction of molecular vibrations with infrared light and identifies the chemical components of the analyzed substance by identifying functional groups (Mohamed et al., 2017).

Fire investigations are inherently complex and challenging processes. The fire itself can destroy or alter crucial physical evidence vital for determining the origin and cause of the blaze. Furthermore, the resulting debris and damage pose significant health and safety risks to investigative teams, making effective scene examination considerably more difficult. In fire scene investigation, the starting point and cause of the fire must be determined in order to reveal the material reality of the incident (Kuloğlu et al., 2020). To determine the cause of a fire, the first ignited material and its location, called the point of origin, must be identified first (Stauffer et al., 2006b). Many studies have focused on the determination of accelerants and fabrics based on FTIR spectra. In 2005, Borusiewicz et al. (2006) investigated how different factors like the type of burned material, type of accelerant, length of time between lighting and extinguishing of fire and the air availability

level affect the detection of accelerant residues in conditions similar to real fires, and the results showed that the first most influential factor was the type of burnt fabric, while the third factor was the type of accelerator. Jais et al. (2020) burned various types of fabrics (cotton, wool, silk, rayon, satin, and polyester) with gasoline and diesel and detected different types of accelerators from the burned fabrics using ATR-FTIR spectroscopy and Principal Component Analysis (PCA) and LDA analyses. They concluded that ATR-FTIR spectroscopy and the PCA method alone was insufficient in the classification of accelerators, but when combined with LDA, the classification success reached 77.8%, and thus different accelerators could be better distinguished in forensic analysis. Peets at al. (2017) examined 26 different single and two-component textile materials and showed that ATR-FTIR spectra combined with chemometric methods such as PCA and discriminant analysis can classify samples with some limitations (e.g. cotton-linen, silk-wool), while statistical discriminant analysis provides a better separation and a complete separation is achieved with the support of optical microscopy; however, for mixed fibers, only approximate composition determination was possible due to structural heterogeneity. Aljannahi et al. (2022) investigated multivariate statistical methods combined with machine learning classification models to classify 138 synthetic textile fibers by FTIR Spectroscopy, applied pre-processing (Savitzky-Golay first derivative, SNV), PCA for pattern recognition and SIMCA for classification and reported that they achieved 97.1% correct classification of test samples at 5% significance level.

Ferreiro-González et al. have developed a rapid analytical method based on the empty space-mass spectrometry electronic nose (E-Nose) for the analysis of Ignitable Liquid Residues (ILRs). Chemometric techniques, including hierarchical cluster analysis (HCA) and linear discriminant analysis (LDA), were utilized on the mass spectrometry data (45–200 m/z) to identify the most effective spectroscopic features for differentiating various ignitable liquids. The refined method was then tested on a collection of fire debris samples. To mimic post-burn conditions, multiple ignitable liquids (gasoline, diesel, citronella, kerosene, paraffin) were used to ignite different materials (wood, cotton, cork, paper, and paperboard). Discriminant analysis achieved complete separation among the samples which can be considered a green technique for fire debris analysis (Ferreiro-González et al., 2016).

In this study, six types of fabric samples (wool, cotton, polyester, polyacrylic, polyamide and acetate) were individually burned with four different ignitable liquids (kerosene, synthetic thinner, 96% ethanol, and 95 octane gasoline). The burning process was performed twice to enhance reliability. Subsequently, FTIR spectra were obtained for all the resulting burned fabric samples, as well as for unburned fabric samples and fabric samples burned without an ignitable liquid. The aim was to determine the ignitable liquids used in the burned fabric residues by comparing these spectra and with the aid of the PCA method applied to the spectra.

The advantages of the method used in this study over the GC-MS method, the gold standard used in forensic fire investigation, are that while GC-MS analysis requires auxiliary gases and chemicals, FTIR requires nothing additional for analysis, making it more economical. Furthermore, while GC-MS is destructive, FTIR is non-destructive, allowing samples to be stored after analysis. While GC-MS is large and stationary, the portable size of FTIR is beneficial for field work.

2. Material and methods

2.1 Samples

Gasoline was obtained from a gas station. Kerosene, alcohol and thinner were purchased from stores that sells chemicals in Istanbul, Türkiye. Multifiber Adjacent Fabric was used for experimental studies which was purchased from Testfabrics Inc. The Multifiber Adjacent Fabric contains six different fabrics, including wool (worsted), spun polyacrylic (orlon 75), spun polyester (dacron 54), spun polyamide (nylon 6.6), bleached cotton and filament acetate in 1.5 cm strips, and all strips adjacent to each other form a 10 cm width of the fabric. A compact portable FTIR analyzer from Uskudar University Department of Forensic Sciences was used to analyze the samples.

2.2 Sample preparation

While preparing the fabric samples, 1 cm x 5 cm strips were cut from each strip of Multifiber Adjacent fabric. The scissors used for this process were sterilized with 70% isopropyl alcohol and it was ensured that

the alcohol evaporated completely to prevent alcohol residue from remaining and affecting the test results. Since the fabrics would be re-burned twice with 4 different accelerants, burned without any ILs, and an unburned control sample from each fabric type would be used, 10 samples were cut from each fabric type. The cut fabric samples were separated according to their types and placed in ziplock bags.

2.3 Burning procedure

The experiment was carried out in a well-ventilated, fire-permitting indoor environment to eliminate wind variability. Before starting the experiment, necessary precautions were taken against a possible fire and protective equipment was used during the experiment. The combustion test was carried out on 20 March 2025, at 10°C air temperature and 60% humidity at the Basaksehir Organized Industrial Site/Istanbul. 50 ml of IL was filled into a 100 ml beaker and the fabric sample to be burned was kept in this beaker for 10 seconds to allow the fabric to absorb the IL. At the end of the period, the fabric sample was removed and waited until it stopped dripping, then placed in the glass petri dish. Samples were lit with a long-neck lighter to prevent hand burns. The experiment was repeated separately with all fabric types and all ILs. In addition, 6 types of fabric were burned with just a lighter without adding any IL. A separate beaker was used for each IL. All beakers were labeled with a permanent marker according to IL. To prevent contamination, all burning processes were carried out in separate glass petri dishes and after waiting for these dishes to cool completely, they were closed with lids and stored until the analysis stage. The samples were taken for analytical examination the next day without waiting for a long time.

2.4 Method

48 samples of burnt fabrics, 6 samples of fabric burned without IL and 6 samples of unburned fabrics were examined by using FTIR. The crystal was cleaned with 70% ethanol after each measurement. The FTIR result of each sample was recorded by adding the experiment number to the codes given to the fabric sample and IL sample type; Fabric types were named according to the order Multifiber Adjacent Fabric; Wool: S1, Poliacrylic: S2, Polyester: S3, Polyamide: S4, Cotton: S5 and Acetate: S6. IL samples were also assigned codes; Kerosene: K, Thinner: T, Alcohol: E, Gasoline: G. (Table 1). The samples in the first burning experiment were coded as '1fabrictypeIL', the samples in the second burning experiment were coded as '2fabrictypeIL', the samples of fabric burned without IL coded as ‘fabrictypeX' and the unburned fabric samples were coded as 'fabrictype'. The FTIR spectrum of all fabric samples was determined. Spectra were recorded in the wavenumber range of 4000–400 cm^{-1}, at 4 cm^{-1} resolution, and 32 scans were averaged for each sample. Samples were taken from three different points and compared in order to obtain good reproducibility.

Table 1. Nomenclature of samples

Sample	Fabric structure	Liquid code	Liquids
S1	Wool	K	Kerosene
S2	Polyacrylic	T	Thinner
S3	Polyester	E	Ethanol
S4	Polyamide	G	Gasoline
S5	Cotton		
S6	Acetate		

For PCA analysis, the average of the FTIR spectra of 2 replicates of each sample was taken and smoothed by applying a 35-point Savitzky-Golay filter. The obtained data were organized in an excel file in the form of a wavenumber-absorption matrix. Each spectrum was given as a row; the absorbance value corresponding to each wavenumber was given as a column. This excel file was transferred to the OriginPro 2025 program and the analysis was performed in this program. PCA components were calculated automatically and "scores plot" graphics were created over the first two components with the highest variance (PC1 and PC2).

3. Results and discussion

3.1 FTIR analysis

3.1.1 S1-Wool

Wool is a fiber characterized by peptide bases, mainly consisting of amino acids; although its composition can vary, it is characteristically recognized by its amide bands (Nayak et al., 2012). The FTIR spectrum of the unburned wool fabric (S1) displays a broad OH/NH stretching band in the range of 3300–3400 cm^{-1}, attributed to hydrogen bonding within the keratin structure. Aliphatic C–H stretching vibrations originating from the side chains of keratin are observed between 2925–2850 cm^{-1}. A strong absorption band at 1650 cm^{-1}, corresponding to the Amide I band (C=O stretching), is evident, along with a peak at 1540 cm^{-1} (Amide II band), which results from a combination of N–H bending and C–N stretching vibrations. Additionally, a peak at 1230 cm^{-1}, assigned to the Amide III band, reflects combined N–H and C–N vibrations.

In the FTIR spectrum of the thermally degraded wool fabric (S1X), the N–H/O–H stretching band around 3300 cm^{-1} is significantly weakened, indicating the disruption of hydrogen bonding. The Amide I and II bands are also reduced in intensity, consistent with the degradation of keratin polypeptide chains. The presence of weakened, yet characteristic bands in the 1600–1700 cm^{-1} region suggests the formation of carbonization products (pyrolytic C=O), typical of thermal decomposition (Wang et al., 2021). The FTIR spectrum of S1K reveals CH_2/CH_3 asymmetric and symmetric stretching vibrations in the range of 2948–2872 cm^{-1}, indicative of aliphatic hydrocarbon residues. Furthermore, peaks at 1460 cm^{-1} and 1375 cm^{-1}, corresponding to CH_2 scissoring and CH_3 bending modes respectively, confirm the presence of methyl and methylene structures. The FTIR spectrum of S1T exhibits aromatic C=C stretching bands in the 1600–1500 cm^{-1} range, along with out-of-plane C–H bending vibrations between 800–820 cm^{-1}. These findings are characteristic of aromatic compounds such as toluene and xylene, which are commonly found in synthetic thinners, indicating the retention of aromatic residues after combustion.

In the FTIR spectrum of the sample burned with ethyl alcohol (S1E), a broad O–H stretching band around 3300 cm^{-1} is observed, along with pronounced C–O stretching bands between 1050–1100 cm^{-1} (Martín-Alberca et al., 2018). These features suggest partial oxidation and the presence of residual alcohol-derived compounds post-combustion. The FTIR spectrum of S1G (wool fabric burned with gasoline) displays aliphatic CH_2/CH_3 stretching bands in the 2950–2850 cm^{-1} range and a CH_2 bending peak around 1460 cm^{-1}. The weak intensity of C=C stretching bands confirms the predominantly aliphatic nature of gasoline. These results indicate that gasoline, composed mainly of short-chain alkanes, produces lower-intensity aliphatic signals compared to heavier hydrocarbons like kerosene. While the amide bands are partially preserved in the S1E spectrum, the amide bands have significantly decreased in the S1K, S1T and S1G spectra, this indicates the degradation of the protein structure of wool (Socrates, 2004) (Figure 1).

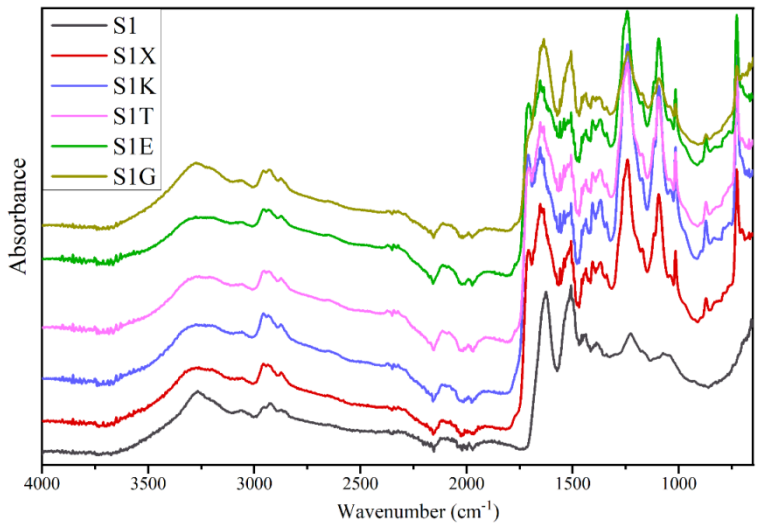

Figure 1. FTIR spectra of wool samples.

3.1.2 S2-Spun polyacrylic (Orlon 75)

Orlon is a trademark name developed by DuPont, Orlon 75 refers to an acrylic fiber with a 75% polyacrylonitrile (PAN) ratio. Polyacrylonitrile is a polymer with the basic repeating unit –CH_2–CH(CN)– and containing a nitrile (–C≡N) group and has strains in the FTIR spectrum that show its monomeric structure and aliphatic skeleton (Li, 2007).

When the FTIR spectrum of the S2 (unburned polyacrylic fabric) sample is examined (Figure 2), the C≡N stretching band in the 2240–2250 cm^{-1} range, which is the characteristic peak of the polyacrylonitrile (PAN) structure, aliphatic C–H stretching in the 2940–2850 cm^{-1} region, and CH_2 bending/scissoring vibrations in the 1450–1380 cm^{-1} range were observed, these bands indicate that the aliphatic structure of the polymer is preserved. For S2X (polyacrylic fabric burned without accelerant), it was observed that the C≡N peak around 2240 cm^{-1} was weakened, this indicates that the nitrile chain was broken due to thermal degradation, in addition, new broad bands indicating aromatic structures were detected around 1600–1650 cm^{-1} in the spectrum. For S2K (polyacrylic fabric burned with kerosene), the CH_2 stretching peaks in the 2950–2850 cm^{-1} region, an increase in CH_2/CH_3 bending peaks at 1460 cm^{-1} and 1375 cm^{-1} was also observed, indicating the contribution of aliphatic hydrocarbon residues from the kerosene. Although the C≡N band specific to the polyacrylonitrile (PAN) structure was weakened, its presence still indicates that the chain structure of the fabric is partially preserved. It was noted that the long-chain hydrocarbon structure of kerosene caused a significant increase in the C–H regions. For S2T (polyacrylic fabric burned with thinner), aromatic C=C stretching in the 1600–1500 cm^{-1} range and aromatic C–H bending around 820 cm^{-1} were observed, this indicates the presence of aromatic solvents in the structure of the thinner. Most importantly, the complete disappearance of the -C≡N band shows that the thinner strongly broke the PAN chain, these findings indicate that aromatic solvents form characteristic bands in FTIR spectra and can disrupt the structure of the nitrile chain.

When the FTIR spectrum of the S2E (polyacrylic fabric burned with ethyl alcohol) sample is examined, the observation of an O–H stretching band around 3300 cm^{-1} indicates alcohol residue or groups formed as a result of oxidation, while the observation of a C–O stretching band in the 1040–1100 cm^{-1} range shows that the alcoholic structure is preserved, the presence of these bands indicates that ethyl alcohol caused an oxidative effect on the PAN structure, in addition, a significant decrease in the -C≡N band was observed. When the FTIR spectrum of the S2G (polyacrylic fabric burned with gasoline) sample is examined, a significant increase in CH_2/CH_3 stretching peaks in the 2950–2850 cm^{-1} region indicates the presence of short-chain hydrocarbons in the gasoline, while the substantial loss of the -C≡N peak indicates that the backbone structure was degraded at high temperatures (Socrates, 2004) (Figure 2).

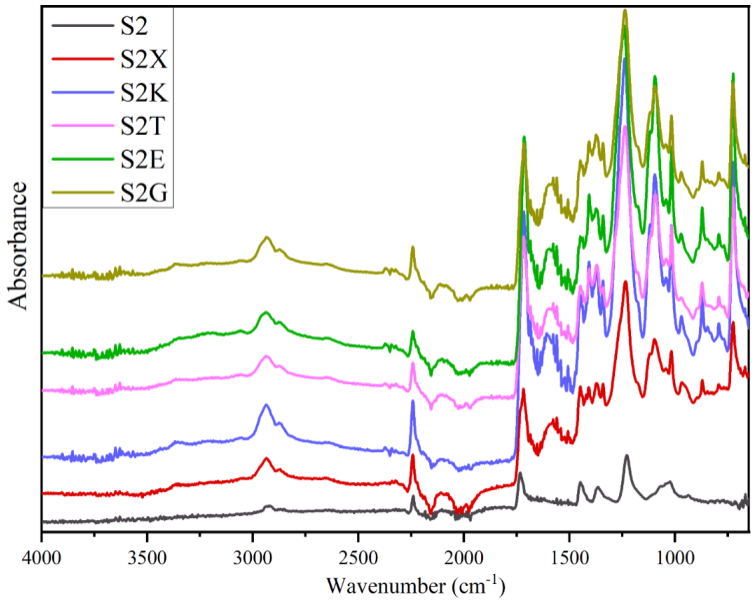

Figure 2. FTIR spectra of polyacrylic samples.

3.1.3 S3- Spun polyester (Dacron 54)

Dacron is also a trademarked name developed by DuPont, Dacron 54 is a type of synthetic fiber produced from polyethylene terephthalate (PET) polymer and contains an aromatic ester structure (Mather et al., 2023).

When the FTIR spectrum of the S3 (unburned polyester fabric) sample is examined (Figure 3), the main bands characterizing its structure were clearly observed. In the 1715–1725 cm^{-1} region, the C=O stretching peak of the aromatic ester carbonyl group was prominent, at 1240–1260 cm^{-1} the C–O stretching, around 1100 cm^{-1} the asymmetric C–O–C stretching peak, in the 870–730 cm^{-1} range the aromatic C–H out-of-plane bending indicating the aromatic structure, and in the 2950–2850 cm^{-1} region the C–H stretching (CH_2 groups) from the aliphatic backbone of the polyester were observed. These results show that the FTIR spectrum of polyester fibers contains carbonyl (ester) group and aromatic characteristic bands originating from terephthalic acid. For S3X, a shift in the original C=O band towards 1710 cm^{-1} and the emergence of new peaks around 1600–1650 cm^{-1} after burning indicate the formation of carbonyl structures due to heat-induced structural degradation, in addition, the weakening of aromatic bands in the 800–750 cm^{-1} region indicates that the ring structures of the fabric were damaged. For S3K, a significant increase was observed in the 2950–2850 cm^{-1} band and in the CH_2/CH_3 bending peaks at 1460 cm^{-1} and 1375 cm^{-1}, this situation arises from the aliphatic hydrocarbon signals of the kerosene, on the other hand, the characteristic aromatic ester peaks of polyester (1720 cm^{-1} and 1250 cm^{-1}) were slightly weakened, indicating that the polymer structure was partially degraded. For S3T, aromatic C=C stretching peaks became prominent in the 1600–1500 cm^{-1} range and aromatic C–H bending peaks formed around 800 cm^{-1}, this indicates the presence of aromatic components such as toluene and xylene in the structure of thinner. The aromatic nature of thinner interacts with the polyester's own aromatic rings, forming overlapping but degraded bands in the FTIR spectrum. For S3E (polyester fabric burned with ethyl alcohol) sample, the observation of a C–O stretching band in the 1050–1100 cm^{-1} range and a broad O–H stretching band around 3300 cm^{-1} indicates the presence of alcohol residue, the characteristic ester carbonyl band of polyester (1720 cm^{-1}) remained in place, but a decrease in its intensity was observed, which shows that the ester groups were not completely decomposed but only slightly damaged. When the FTIR spectrum of the S3G (polyester fabric burned with gasoline) sample is examined, a significant increase in the CH_2/CH_3 stretching peaks in the 2950–2850 cm^{-1} range clearly indicates the presence of short-chain hydrocarbons from gasoline, it was determined that there was a severe loss in the characteristic ester peaks of polyester (1720 cm^{-1}), which indicates that the polyester structure was seriously degraded due to high-temperature burning (Socrates, 2004) (Figure 3).

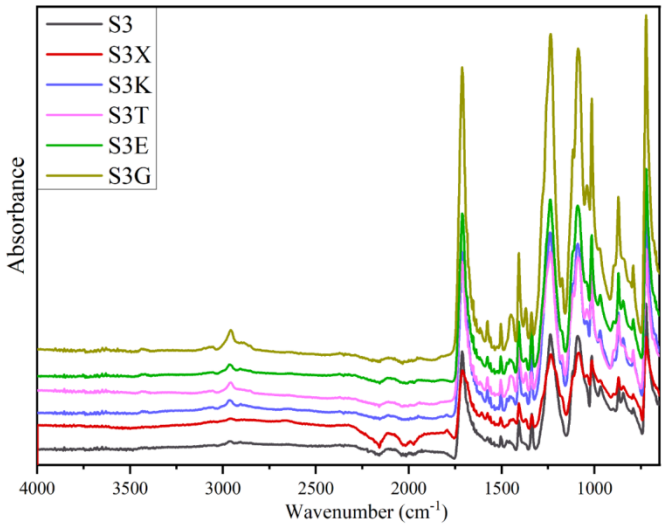

Figure 3. FTIR spectra of polyester samples.

3.1.4 S4- Spun polyamide (nylon 6.6)

Nylon 6.6 is an aliphatic polyamide based on synthetic origin obtained through polycondensation, and shows typical protein-like peaks such as Amide I, Amide II, and Amide III in FTIR spectra (Smith, 2011). As the

FTIR spectrum of the S4 sample (unburned polyamide fabric) (Figure 4), characteristic absorption bands of the polyamide structure were observed. A broad N–H stretching vibration appears at approximately 3300 cm^{-1}, attributed to hydrogen-bonded amide groups. The CH_2 asymmetric and symmetric stretching bands are present at 2930 cm^{-1} and 2850 cm^{-1}, respectively. The Amide I band is observed in the 1630–1650 cm^{-1} range, while the Amide II band appears around 1540 cm^{-1}. Additionally, bands corresponding to Amide III vibrations are present in the 1200–1300 cm^{-1} region. The pronounced N–H stretching and the combination of Amide I and II bands are indicative of the well-ordered polyamide chain structure (Pavia et al., 2014; Vartiainen et al., 2004). In the FTIR spectrum of the S4X sample (polyamide fabric burned without accelerant), a significant reduction in the intensity of the N–H stretching band at 3300 cm^{-1} and the Amide I and II bands is observed. This suggests the disruption of hydrogen bonding and extensive degradation of the polymer chains due to thermal exposure. For the S4K sample (polyamide fabric burned with kerosene), the FTIR spectrum reveals a notable increase in C–H stretching vibrations within the 2950–2850 cm^{-1} range and in CH_2/CH_3 bending vibrations at 1460 cm^{-1} and 1375 cm^{-1}. These findings indicate the presence of long-chain aliphatic hydrocarbon residues derived from kerosene. A slight weakening of the amide bands suggests that the polyamide backbone is only partially degraded. The FTIR spectrum of the S4T sample (polyamide fabric burned with thinner) exhibits distinct aromatic C=C stretching bands between 1600–1500 cm^{-1} and aromatic C–H out-of-plane bending bands in the 800–820 cm^{-1} region. These peaks confirm the presence of aromatic compounds such as toluene and xylene, components of thinner. Furthermore, the suppression of Amide I and II bands suggests degradation of the polyamide structure. In the spectrum of the S4E sample (polyamide fabric burned with ethyl alcohol), a broad O–H stretching band near 3300 cm^{-1} and a C–O stretching band in the 1040–1100 cm^{-1} range are observed, indicating residual alcohol. The slight reduction in amide peak intensity implies partial degradation of the nylon structure under high thermal conditions. Finally, the FTIR spectrum of the S4G sample (polyamide fabric burned with gasoline) shows increased CH_2/CH_3 stretching vibrations in the 2950–2850 cm^{-1} range and an intensified CH_2 bending band at 1460 cm^{-1}, reflecting the presence of short-chain aliphatic hydrocarbons from gasoline. The near-complete disappearance of the Amide I and II bands indicates severe degradation of the polyamide chains due to high-temperature combustion (Socrates, 2004) (Figure 4).

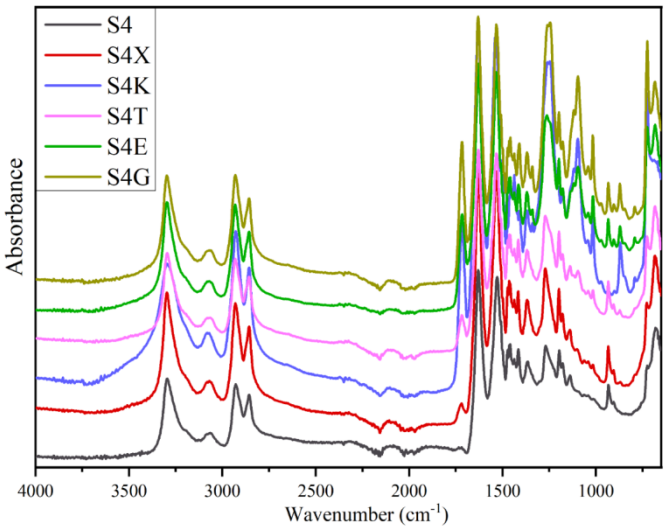

Figure 4. FTIR spectra of polyamide samples.

3.1.5 S5- Bleached cotton

Cotton is primarily composed of cellulose, which can be identified in FTIR spectra by distinct O–H, C–H, and C–O vibrational bands (Peets et al., 2017; Williams, 2018).

The FTIR spectrum of the S5 sample (unburned cotton fabric) shows characteristic peaks associated with cellulose. A broad O–H stretching band is observed in the 3330–3400 cm^{-1} range due to hydrogen bonding, along with a C–H stretching band corresponding to aliphatic CH_2 groups at 2900 cm^{-1}. Additional peaks include a CH_2 scissoring vibration at 1429 cm^{-1}, a C–H bending vibration at 1370 cm^{-1}, and asymmetric C–O–C stretching bands (indicative of glycosidic linkages) in the 1160–1050 cm^{-1} region. A distinct O–H

bending peak from adsorbed water is also seen at 1640 cm^{-1}. Importantly, the peak at 895 cm^{-1}, attributed to β-glycosidic bond stretching, is characteristic of cellulose and confirms the cotton structure.

For S5X sample (cotton fabric burned without an accelerant), a significant weakening of the O–H stretching band near 3300 cm^{-1} and the disappearance of C–O and β-glycosidic bond signals indicate extensive thermal degradation. These changes suggest the breakdown of hydrogen bonds and cleavage of glycosidic linkages. Additionally, the emergence of a broad band around 1600 cm^{-1} is indicative of aromatic structures formed during carbonization. The S5K sample (cotton fabric burned with kerosene) displays an increase in CH_2/CH_3 stretching peaks in the 2950–2850 cm^{-1} region and enhanced C–H bending vibrations between 1460–1375 cm^{-1}. These features point to the presence of aliphatic hydrocarbons derived from kerosene. Although cellulose-related bands are diminished, the persistence of the β-glycosidic peak suggests that the glycosidic structure is only partially degraded. For the S5T sample (cotton fabric burned with thinner), the presence of aromatic C=C stretching bands in the 1600–1500 cm^{-1} range and an aromatic C–H out-of-plane bending vibration at 820 cm^{-1} indicates components such as toluene and xylene, typically found in thinner (Silverstein et al., 2005). The disappearance of C–O–C and β-glycosidic peaks demonstrates that thinner induces complete degradation of the glycosidic structure in cellulose. O–H stretching band around 3300 cm^{-1} and the C–O stretching band within 1050–1100 cm^{-1} suggests that ethyl alcohol may be physically adsorbed onto the fabric surface. Moreover, the presence of the characteristic β-glycosidic bond signal at 895 cm^{-1} implies that the cellulose structure remains largely intact, and degradation is minimal. S5G sample (cotton fabric burned with gasoline) exhibits a marked increase in aliphatic C–H stretching vibrations between 2950–2850 cm^{-1}, indicating the presence of gasoline residues. However, the near-complete disappearance of cellulose-related peaks, particularly the β-glycosidic and C–O bands, reveals that gasoline causes extensive degradation of the cotton structure, with little to no detectable cellulose remaining in the FTIR spectrum (Socrates, 2004) (Figure 5).

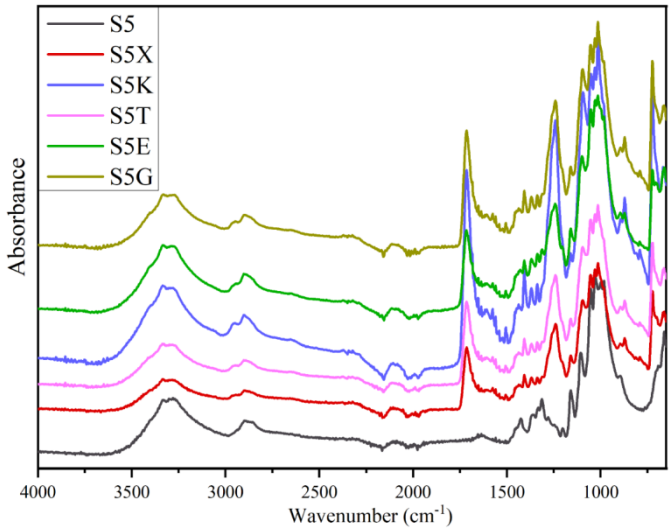

Figure 5. FTIR spectra of cotton samples.

3.1.6 S6- Filament acetate

Cellulose acetate is a polymer obtained by acetylation of cellulose. In the FTIR spectrum of cellulose acetate, O-H vibration bands are seen around 3300 cm^{-1} and 2900 cm^{-1} and C=O vibration band is seen around 1700 cm^{-1} (Huda et al., 2019).

When the FTIR spectrum of the S6 (unburned cellulose acetate fabric) sample is examined (Figure 6), characteristic structural bands of cellulose acetate are observed, including a strong and diagnostic C=O stretching peak at 1740 cm^{-1} belonging to the carbonyl group of the acetate, C–H stretching peaks at 2950–2850 cm^{-1} from CH_3 and CH_2 groups, C–H bending at 1368 cm^{-1} from the CH_3 group, C–O stretching bands at 1225 cm^{-1} and 1040 cm^{-1} corresponding to ester and ether functions, and a β-glycosidic bond vibration at 897 cm^{-1} related to the cellulose backbone. This spectrum identifies the acetylated cellulose structure with the strong carbonyl signal at 1740 cm^{-1} and shows the glycosidic peaks of the cellulose skeleton.

For S6X (cellulose acetate fabric burned without accelerant), a decrease in the C=O peak at 1735 cm^{-1} as well as in the C–O peaks and β-glycosidic bond peak that form the basis of the cellulose acetate structure is observed. This indicates that the acetate groups were degraded by heat and that the glycosidic bonds were broken, showing that the structure was significantly degraded. A new and broad band appearing around 1600 cm^{-1} in the spectrum indicates the formation of conjugated carbon structures after burning. For S6K (cellulose acetate fabric burned with kerosene), a significant increase is observed in the C–H stretching peaks in the 2950–2850 cm^{-1} range and in the CH_2/CH_3 bending signals in the 1465–1375 cm^{-1} range, indicating the presence of hydrocarbons from kerosene. The C=O band still being observable indicates that although thermal degradation of the polymer has begun, the structure remains identifiable. When the FTIR spectrum of the S6T (cellulose acetate fabric burned with thinner) sample is examined, the presence of aromatic C=C stretching peaks in the 1600–1500 cm^{-1} range and the aromatic C–H out-of-plane bending peak at 820 cm^{-1} indicates the presence of aromatic components such as toluene and xylene in the thinner. The suppression of C=O and C–O signals indicates that the aromatic solvents have disrupted the polymer chain. For S6E (cellulose acetate fabric burned with ethyl alcohol), a broad O–H stretching band around 3300 cm^{-1} and C–O stretching peaks in the 1050–1100 cm^{-1} range indicates the presence of alcohol residues. The weakening of the C=O band suggests that contact with ethanol caused slight degradation of the acetate groups. When the FTIR spectrum of the S6G (cellulose acetate fabric burned with gasoline) sample is examined, distinct aliphatic C–H stretching peaks in the 2950–2850 cm^{-1} range and signals related to aromatic and carbonized structures at 1600 cm^{-1} are observed, indicating the presence of gasoline residues. The near-complete disappearance of C=O and C–O signals indicates the extent of thermal degradation. In fabrics burned with ethanol, C–O stretching in the 1050–1100 cm^{-1} region and broad O–H stretching signals around 3300 cm^{-1} showed an increase, revealing that alcohol left molecular residues after combustion. In samples where gasoline was used, both the aliphatic C–H regions became stronger, and there was a significant suppression of natural structural signals, such as those from protein or cellulose. Crucially, the absence of these signals in unburned control samples and those burned without ignitable liquids proves that these specific peaks originate from the applied ignitable liquid and are distinctive (Socrates, 2004) (Figure 6).

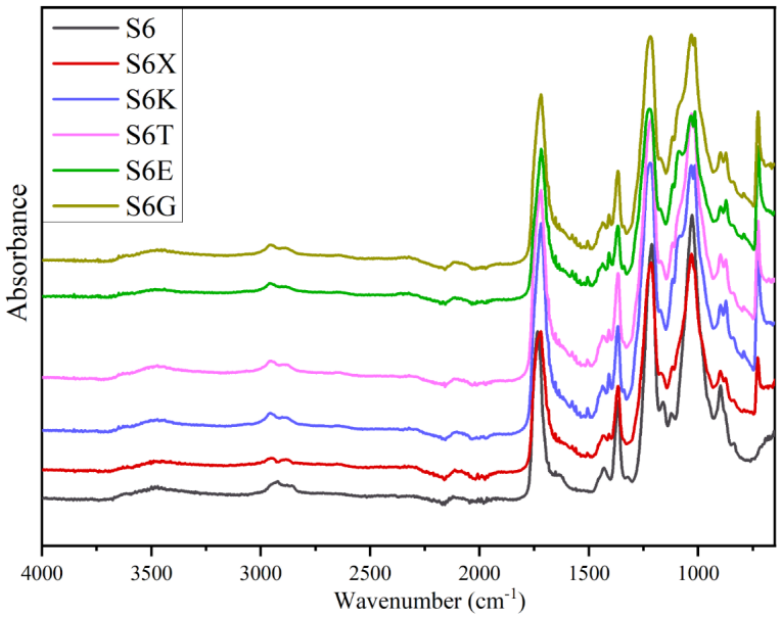

Figure 6. FTIR spectra of cellulose acetate samples.

3.2 PCA

PCA score plot visualizes how samples cluster or distribute relative to each other using two main components (PC1 and PC2), which show a large portion of the variation in the FTIR data of the samples. Orange software was used for this PCA analysis. Before PCA, Orange normalized the data using Z-score standardization. After normalization, the software generated a correlation matrix showing the relationships between the variables. The software extracted the eigenvalues and eigenvectors of the correlation matrix and selected PC1 and PC2, which explained the most variance among the eigenvalues. The analysis was then visualized with a scatter plot.

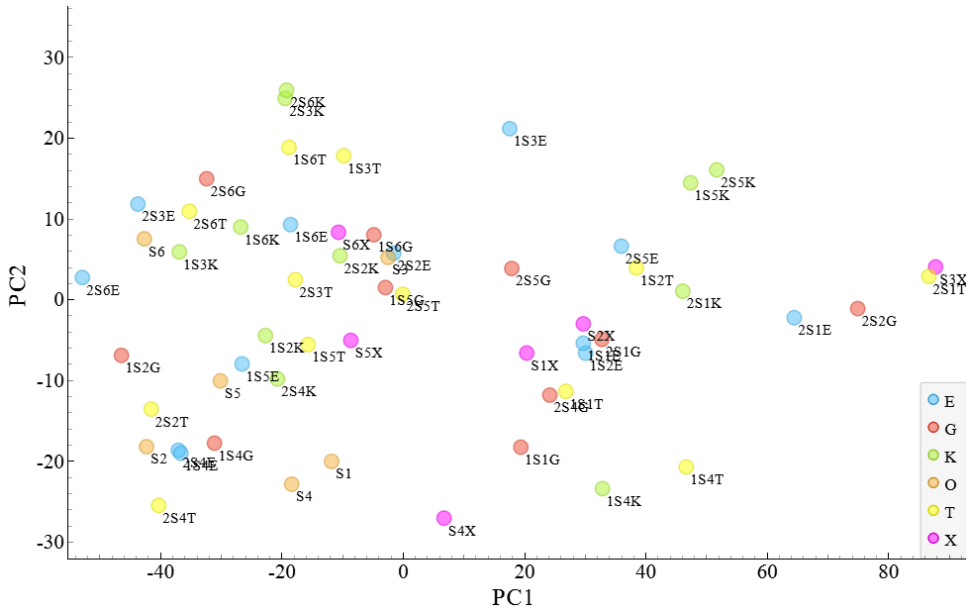

Figure 7. PCA score plot of all samples

It was observed that the PC1 axis explained 68.59% of the total variance, while the PC2 axis explained 11.79% of the total variance. This shows that the main differentiation in the data occurred largely in the PC1 axis and captured the most important chemical changes between the samples. The PC1 axis represents the effect of combustion, providing the fundamental distinction between unburned fabrics and fabrics burned with an igniter. The PC2 axis reflects secondary differentiations such as the degree of combustion, the type of igniter used, or the unique reactions of the fabric itself. Unburned fabrics were observed to cluster on the left side of the graph, generally at negative PC1 values. This indicates that the FTIR values of unburned fabrics are similar to each other and distinctly different from burned samples. Most fabrics burned with different ILs were observed to shift to the right side of the graph, towards positive PC1 values. This indicates that the burning process causes significant changes in the chemical structure of the fabrics. Fabrics burned without an igniter are observed to be positioned between unburned fabrics and fabrics burned with an igniter. This suggests that burning with only a lighter causes some chemical changes in the fabrics, though not as extensive as burning with an igniter. For example, S1X being closer to the unburned group suggests that this fabric underwent less chemical change when burned without an igniter, while S4X being further to the right indicates that S4 fabric underwent significant change even when burned without an igniter. When examining the 1st and 2nd replicates of the same fabric and igniter combination in the PCA score plot, most were found to be quite close to each other. This indicates the reproducibility of the experiment and FTIR measurements. It was observed that although there were minor differences in the absorbances of the FTIR spectra of almost all samples' 1st and 2nd replicates, their spreads along the wavelength axis were the same.

Although the PCA score plot shows how samples cluster based on their spectral similarities, it does not have sufficient discriminatory power to be used alone for the identification of the igniter type. However, when PCA analysis is used in conjunction with FTIR spectra, the probability of correctly identifying the type of IL is significantly increased. This is because certain igniters produce characteristic chemical changes that appear as identifiable peaks in FTIR spectra; for example, aromatic C=C stretching bands observed at approximately 1600 cm^{-1} in burned with thinner samples or concentrated aliphatic C–H bands seen in fabrics burned with gasoline or kerosene. These spectral fingerprints help explain the positional separation of samples in the PCA plot and provide important insights into the chemical effects of combustion. Therefore, combining PCA analysis with FTIR spectral interpretation leads to more reliable data evaluation and increases the accuracy of IL identification.

4. Conclusion

In this study, a total of 60 samples, consisting of six different textile fabrics (wool, polyacrylic, polyester, polyamide, cotton and acetate) burned with four different ignitable liquids (gasoline, synthetic thinner, ethanol, kerosene), alongside unburned and burned without accelerants, were analyzed using FTIR

spectroscopy, and the resulting data was classified with PCA. The analyses determined that each ignitable liquid left distinguishable chemical traces on the fabrics with its unique characteristic FTIR bands. Kerosene was identified across all fabric types by aliphatic C–H bands in the 2950–2850 cm^{-1} range and CH_2/CH_3 bending bands in the 1460–1375 cm^{-1} range. Synthetic thinner, on the other hand, was characterized by aromatic C=C bands at 1600–1500 cm^{-1} and aromatic C–H bands at approximately 820 cm^{-1}, particularly in wool, polyacrylic, polyester, cotton, and acetate fabrics. Ethanol was detected, especially in cellulosic fabrics, by O–H bands at 3300 cm^{-1} and C–O bands at 1050–1100 cm^{-1}. Gasoline led to an increase in CH_2/CH_3 stretching bands at 2950–2850 cm^{-1} and a loss of specific bands originating from protein/cellulose across all fabrics. PCA analysis explained approximately 68% of these spectral changes through the PC1 component. While PCA analysis provided a clear distinction between burned and unburned samples, it could not cluster the ignitable liquid types individually. However, it was concluded that the combined use of PCA with FTIR allows for a more systematic interpretation of spectral differences. Consequently, the study demonstrates that FTIR and PCA methods, when used together, can be evaluated as a rapid, non-destructive, repeatable, and supportive analytical method for ignitable liquid detection in forensic fire investigations. As an aspect of the study that is open to improvement, it is suggested that combining the analysis method proposed in this study with LDA analysis can increase the accuracy rate.

Author contribution

S.K: writing, original draft, methodology, investigation, visualization, conceptualization, supervision, review, funding and editing B.I.Y: writing, original draft, methodology, investigation, visualization, conceptualization S.A: writing, methodology, conceptualization, review and editing.

Declaration of ethical code

The authors of this article declare that the materials and methods used in this study do not require ethics committee approval and/or legal-special permission.

Conflicts of interest

The authors declare that they have no conflict of interest.

References

Aljannahi, A., Alblooshi, R. A., Alremeithi, R. H., Karamitsos, I., Ahli, N. A., Askar, A. M., Albastaki, I. M., Ahli, M. M., & Modak, S. (2022). Forensic analysis of textile synthetic fibers using a FT-IR spectroscopy approach. *Molecules, 27*(13), 4281. https://doi.org/10.3390/molecules27134281

Association of British Insurers. (2004). *Memorandum by the Association of British Insurers (ABI) (FIR 59)*. [Presented to Office of the Deputy Prime Minister: Housing, Planning and Local Government Committee]. U.K. Parliament. https://publications.parliament.uk/pa/cm200304/cmselect/cmodpm/43/43we06.htm

Balch, J. K., Bradley, B. A., Abatzoglou, J. T., Nagy, R. C., Fusco, E. J., & Mahood, A. L. (2017). Human-started wildfires expand the fire niche across the United States. *Proceedings of the National Academy of Sciences of the United States of America, 114*(11), 2946–2951. https://doi.org/10.1073/pnas.1617394114

Borusiewicz, R., Zięba-Palus, J., & Zadora, G. (2006). The influence of the type of accelerant, type of burned material, time of burning and availability of air on the possibility of detection of accelerants traces. *Forensic Science International, 160*(2–3), 115–126. https://doi.org/10.1016/j.forsciint.2005.08.019

Burton, P. R. S., McNiel, D. E., & Binder, R. L. (2012). Firesetting, arson, pyromania, and the forensic mental health expert. *The Journal of the American Academy of Psychiatry and the Law, 40*(3), 355–365.

CNBC. (2024). *French rail network hit by arson, canceling trains on eve of Olympics.* https://www.cnbc.com/2024/07/26/french-rail-network-hit-by-arson-canceling-trains-on-eve-of-olympics.html

Drysdale, D. (2011). *An introduction to fire dynamics* (3rd ed.). Wiley. https://doi.org/10.1002/9781119975465

Evans-Nguyen, K., & Hutches, K. (Eds.). (2019). *Forensic analysis of fire debris and explosives*. Springer International Publishing. https://doi.org/10.1007/978-3-030-25834-4

Federal Bureau of Investigation. (2024). *Uniform Crime Reporting Program Data: Arson, United States, 2022*. Inter-university Consortium for Political and Social Research. https://doi.org/10.3886/ICPSR39064.v1

Ferreiro-González, M., Barbero, G. F., Palma, M., Ayuso, J., Álvarez, J. A., & Barroso, C. G. (2016). Determination of ignitable liquids in fire debris: Direct analysis by electronic nose. *Sensors, 16*(5), 695-706. https://doi.org/10.3390/s16050695

Hall, C. (1988). Arson and its management in NSW. *Australian Journal of Management*, *13*(1), 31–51. https://doi.org/10.1177/031289628801300102

Houck, M. M. (2009). *Identification of textile fibers*. Woodhead Publishing.

Huda, E., Rahmi, R, & Khairan, K. (2019). Preparation and characterization of cellulose acetate from cotton. *IOP Conference Series: Earth and Environmental Science, 364*, Article 012021. https://doi.org/10.1088/1755-1315/364/1/012021

Jais, F. I., Syed Mohd Daud, S. M., Mahat, N. A., Ismail, D., & Mohamad Asri, M. N. (2020). Forensic analysis of accelerant on different fabrics using attenuated total reflectance-Fourier transform infrared spectroscopy (ATR-FTIR) and chemometrics techniques. *Malaysian Journal of Medicine and Health Sciences, 16*(2).

Kuloğlu, M., Dağlıoğlu, N., & Kuloğlu, L. (2020). Adli yangın incelemeleri: Sorunlar ve çözüm önerileri. *Journal of Forensic Sciences and Crime Research, 2*(1), 37–58.

Kuppusamy, S., Maddela, N. R., Megharaj, M., & Venkateswarlu, K. (2020). *Total petroleum hydrocarbons: Environmental fate, toxicity, and remediation*. Springer Cham. https://doi.org/10.1007/978-3-030-24035-6

Li, L. C. (2007). Identification of textile fiber by Raman microspectroscopy. *Forensic Science Journal, 6*, 55–62.

Mandal, S., Song, G., Rossi, R. M, & Grover I. B. (2021). Characterization and modeling of thermal protective fabrics under Molotov cocktail exposure. *Journal of Industrial Textiles, 51*, 1150S–1174S. https://doi.org/10.1177/1528083720984973

Martín-Alberca, C., Carrascosa, H., San Román, I., Bartolomé, L., & García-Ruiz, C. (2018). Acid alteration of several ignitable liquids of potential use in arsons. *Science & Justice, 58*(1), 7-16. https://doi.org/10.1016/j.scijus.2017.09.004

Mather, R. R., Wardman, R. H., & Rana, S. (2023). *The chemistry of textile fibres*. Royal Society of Chemistry. https://doi.org/10.1039/9781837670505

Mohamed, M. A., Jaafar, J., Ismail, A. F., & Othman, M. H. D & Rahman M.A. (2017). Ch. 1: Fourier transform infrared (FTIR) spectroscopy. In N. Hilal, A. F. Ismail, T. Matsuura, & D. Oatley-Radcliffe (Eds.) In *Membrane characterization* (pp. 3–29). Elsevier. https://doi.org/10.1016/B978-0-444-63776-5.00001-2

National Fire Protection Association. (2021). *Guide for fire and explosion investigations (NFPA 921:2021)*. Quincy, MA: National Fire Protection Association.

National Fire Protection Association. (2022). *Standard for portable fire extinguishers (NFPA 10:2022)*. Quincy, MA: National Fire Protection Association.

National Fire Protection Association. (2024). *Flammable & combustible liquids code (NFPA 30:2024)*. Quincy, MA: National Fire Protection Association.

Nayak, R., Padhye, R., & Fergusson, S. (2012). Ch. 11: Identification of natural textile fibres. In R. M. Kozlowski & M. Mackiewicz-Talarczyk (Eds.), *Handbook of natural fibres (second edition) volume 1: Types, properties and factors affecting breeding and cultivation* (pp. 314-344). Woodhead Publishing Series in Textiles. https://doi.org/10.1533/9780857095503.1.314

Palmer, D. A. (2024, April 12). Arson charge rates in the UK: Data reveals widespread justice gaps. *International Fire & Safety Journal*. https://internationalfireandsafetyjournal.com/arson-charge-rates-in-the-uk-data-reveals-widespread-justice-gaps/

Peets, P., Leito, I., Pelt, J., & Vahur, S. (2017). Identification and classification of textile fibres using ATR-FT-IR spectroscopy with chemometric methods. *Spectrochimica Acta Part A: Molecular and Biomolecular Spectroscopy, 173*, 175–181. https://doi.org/10.1016/j.saa.2016.09.007

Peterson, A. (2015). *Towards recycling of textile fibers: Separation and characterization of textile fibers and blends* [Master's thesis, Chalmers University of Technology]. Chalmers Publication Library.

Quintiere, J. G. (2006). Introduction to fire. In *Fundamentals of fire phenomena* (Ch. 1, pp. 1–18). Wiley.

Rouessac, F., & Rouessac, A. (2013). *Chemical analysis: Modern instrumentation methods* (2nd ed.). Wiley.

Sampat, A. A. S., Van Daelen, B., Lopatka, M., Mol, H., Van der Weg, G., Vivó-Truyols, G., Sjerps, M., Schoenmakers, P. J., & Van Asten, A. C. (2018). Detection and characterization of ignitable liquid residues in forensic fire debris samples by comprehensive two-dimensional gas chromatography. *Separations, 5*(3), 43. https://doi.org/10.3390/separations5030043

Segal, Y., Gill, G., Yadav, G., Singh, G., & Riess, P. (2024). Unraveling the inferno: An arson case series. *Cureus, 16*(5), e60127. https://doi.org/10.7759/cureus.60127

Silverstein, R. M., Webster, F. X., & Kiemle, D. (2005). *Spectrometric identification of organic compounds* (7th ed.). Wiley.

Smith, B. C. (2011). *Fundamentals of Fourier transform infrared spectroscopy* (2nd ed.). CRC Press. https://doi.org/10.1201/b10777

Socrates, G. (2004). *Infrared and Raman characteristic group frequencies: Tables and charts* (3rd ed.).

Stauffer, E., Dolan, J. A., & Newman, R. (2006a). Chemistry and physics of fire and liquid fuels. In Fire debris analysis (ch. 4, pp. 85–88). Elsevier.

Stauffer, E., Dolan, J. A., & Newman, R. (2006b). Introduction. In Fire debris analysis (ch. 1, pp. 1–17). Elsevier.

U.S. Bureau of Indian Affairs. (2024). Branch of Wildland Fire Management. https://www.bia.gov/bia/ots/dfwfm/bfu

U.S. Fire Administration. (2023). *Annual report to Congress: Fiscal year 2022*.

Wang, H., Guo, S., Zhang, C., Qi, Z., Li, L., & Zhu, P. (2021). Flame Retardancy and Thermal Behavior of Wool Fabric Treated with a Phosphorus-Containing Polycarboxylic Acid. *Polymers*, *13*(23), 4111. https://doi.org/10.3390/polym13234111

Williams, G. A. (2018, May). Forensic textile damage analysis: Recent advances. *Research and Reports in Forensic Medical Science, 8*, 1–8. https://doi.org/10.2147/RRFMS.S166435

Yadav, V. K., Nigam, K., & Srivastava, A. (2020). Forensic investigation of arson residue by infrared & Raman spectroscopy: From conventional to non-destructive techniques. *Medicine, Science and the Law, 60*(3), 206–215. https://doi.org/10.1177/0025802420914807